American Scientific Research Journal for Engineering, Technology, and Sciences (ASRJETS)

ISSN (Print) 2313-4410, ISSN (Online) 2313-4402

http://asrjetsjournal.org/

Structural, Electronic and Optical Properties of $CsMI_3$(M=Ge,Sn,Pb) Perovskite from First Principles

Haoxuan Liu[a]*, Haiming Zhang[b]

[a,b]*Tiangong University School of Physical Science and Technology ,No.399 Binshui West Road Xiqing District, Tianjin300387,China*

[a]*Email: 385313761@qq.com*

[b]*Email: zhmtjwl@163.com*

Abstract

The all-inorganic lead halide perovskites has received wide attention in optoelectronic applications such as solar cells and light-emitting diodes due to its high photoabsorption, suitable bandgap and good stability. Based on the first principles, the electronic structure and optical properties of the structure are studied by substituting all the lead elements in CsPbI3 with Ge and Sn.We found that the structural stability of all the substituted materials was enhanced. The tolerance factors of CsGeI3 and CsSnI3 were 0.934 and 0.874, respectively. The most important point is to replace the toxic Pb element, which not only reduces environmental pollution but also can be more suitable for commercial production. By analyzing the imaginary part of the dielectric function and absorption coefficient, it is found that the blue shift occurs in all the materials which replace Pb element, and the absorption ability of sun light is stronger in the visible light range, which proves the foundation for lead free perovskite solar cells.

Keywords: All inorganic perovskite; first principles; electronic structure; optical properties.

---

* Corresponding author.

1. Introduction

Photoelectric conversion is the direct conversion of light into electricity, so it has the real potential to replace the fossil fuel energy with harmful consequences to nature. In order to prevent environmental pollution, people need to pay attention to clean energy. All-inorganic perovskite materials have been widely studied owing to its high light absorption rate, suitable band gap, and good stability [1,2]. Up to date, the perovskite photoelectric efficiency(PCE)has reached to 25.2% [3].The halide-based perovskite formula is ABX3, and the crystal structure is shown in Figure 1. “X” atoms located in the centers of the cube’s sides are replaced by halogen elements, such as I, Br, Cl. “A”, “B” atoms are located in the center and the corner of the cube, respectively. “B” atoms belong to the fourth group(Ge, Sn, Pb), “A” atom can be positive monovalent metal cation or organic monovalent molecule, we generally use Cs+[4]. In the perovskite material, the BX6 octahedron form at the angle of the cube, causing the direction angle and inclination of the bond affected by various physical conditions, resulting in phase shift and changing the electronic and optical properties of the material. This octahedral joint is more stable, and the gap between atoms is larger, which is conducive to defect migration[5].The photoelectric conversion efficiency of organic-inorganic hybrid perovskite solar cells(PVSKs)is gradually increasing after a lot of research. However, the Pb element contained in it will not only pollute the environment, but also affect the commercial production of perovskite materials. So many researchers have carried out a series of studies on reducing Pb element in perovskite materials. As an effective alternative strategy, B-site substitution(such as Sn2+, Ge2+ to replace Pb2+)is conducive to explore the environmentally friendly PVSKs with reduced Pb2+ concentration[6]. Due to the systematic study of all of the Pb elements be replaced by the fourth main group elements, the study of physical properties of perovskite materials after the replacement is relatively rare, the purpose of this paper is to replace the Pb element with the Ge, Sn element of the fourth main group based on density functional theory, and then systematically study the photoelectric performance and the band gap differences among the CsMI3(M= Ge, Sn, Pb), with the intention of reducing the Pb element in the material[7]. It is discovered that B-position substitution can effectively improve the stability and optical performance of the solar cells, thus promoting its application in solar cells, so as to provide theoretical guidance for the research of the lead-free solar cells.

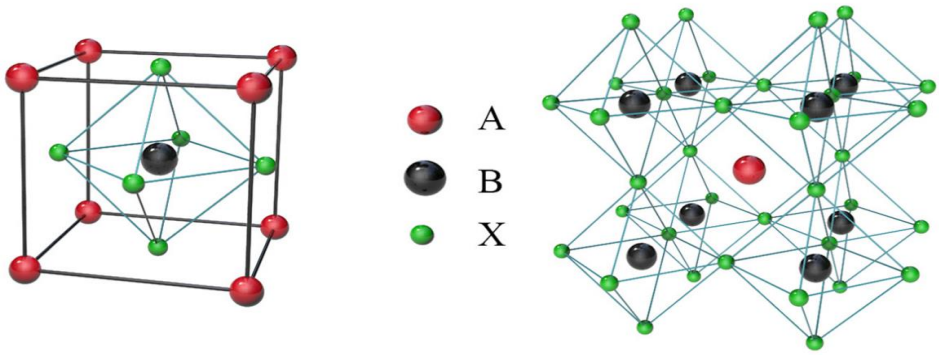

Figure 1: Crystal structure of perovskite material

2. Computational Methods

All first-principles calculations were performed within the framework of plane-wave pseudopotential approach based on the density functional theory(DFT)implemented in the CASTEP code[8].Throughout our calculations, the electron-ion interaction was taken into account by using the "Generated on-the-fly" ultrasoft pseudopotentials[9]while the electronic exchange-correlation interaction was evaluated via the generalized gradient approximation GGA within the Perdew-Burke-Ernzerhof(PBE)scheme[10]. The electronic wave functions were expanded in plane-waves up to a kinetic energy cut-off of 500 eV. A 6×6×6 Monkhorst-Pack grid was employed for sampling of the Brillouin zone. The lattice parameters and the atomic positions were optimized until the forces and the convergence threshold for self-consistent field(SCF)iteration within 0.01 eV/Å and 10−5 eV[11], respectively. CsMI3 (M= Ge, Sn, Pb)unit cells were shown in Figure 2.

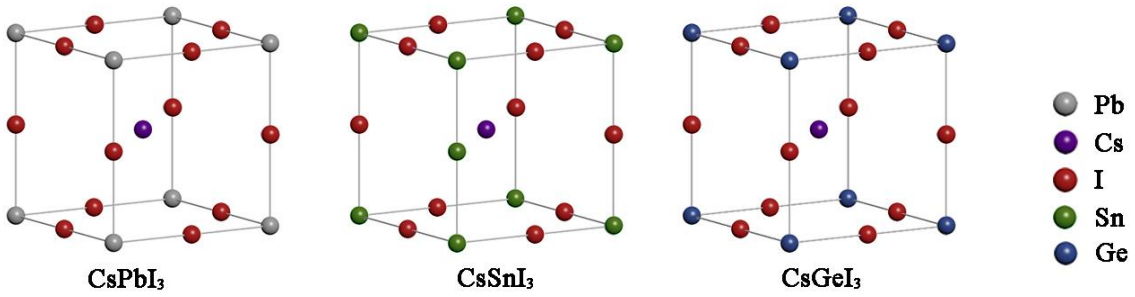

Figure 2: Crystal structure of $CsMI_3$ (M = Ge, Sn, Pb). green, brown, blue, grey, and purple spheres denote Sn, I, Ge, Pb, and Cs, respectively.

3. Results and Discussion

3.1. Structural properties

It is necessary to be mentioned that, in the study of the halide perovskite materials, selection of the A and B atoms are geometrically restricted, we generally use Goldschmidt tolerance factor τ and the formula is:

$$\tau = \frac{r_A + r_X}{\sqrt{2}(r_B + r_X)} \quad (1)$$

Where r_A, r_B, r_X are ionic radii for A, B, and X sites, respectively. The tolerance factor quantitatively gives the matching size of the cavity formed by a cation in BX6 octahedron. When $0.8 \le \tau \le 1$, the material is perovskite structure, when $\tau > 1$ or $\tau < 0.8$, the radius of a cation is too large or too small relative to BX6 octahedron, perovskite material can not be formed[12]. When $\tau = 1$, the structure of perovskite is the most stable. The atomic radii and tolerance factors of Pb, Sn, and Ge are shown in Table 1. It can be seen that the stability of CsMI3(M = Ge, Sn, Pb)decreases with the increase of atomic number. The calculated lattice parameters of CsMI3(M= Ge, Sn, Pb)are given in Table 2. We can see that for CsMI3(M= Ge, Sn, Pb)their lattice parameter increase with the atomic radii increasing. The reason is that the atomic radius increases, so the bond length increases, the bond energy decreases, the lattice constant increases[13]. The lattice distortion is always fundamentally related to the unfavourable value of τ. If the halide anion X didn't change, the B-site bivalent cations determine the site of [BX6]4- octahedral, and thus have an influence on the cubo-octahedral voids for monovalent cations (A+)[14]. For the intrinsic CsPbI3, the Cs + of the unit price is less than the cubic octahedral void site ($\tau = 0.807 < 1$), it results in the rotation and inclination of [BX6]4- octahedrals and reduces the structural stability[15]. Considering that the ion radius of Sn2+ and Ge2+ is smaller than that of Pb2+, they can enlarge the tolerance factor τ of perovskite solar cells(PVSKs). The tolerance factors of CsSnI3 and CsGeI3 are 0.874 and 0.934, respectively, indicating that they suffer less octahedral rotation and distortion than CsPbI3, so their structural stability is higher[16].It is of great significance to promote the commercial production of all-inorganic perovskite solar cells.

Table 1: The Ionic Radii (R_i) and Calculated τ of $CsMI_3$(M= Ge, Sn, Pb)PVSKs

Ion	R_i (Å)	Compounds	τ
Pb^{2+}	1.19	$CsPbI_3$	0.807
Sn^{2+}	0.93	$CsSnI_3$	0.874
Ge^{2+}	0.73	$CsGeI_3$	0.934

Table 2： The Calculated Lattice Parameters of $CsMI_3$(M= Ge, Sn, Pb)PVSKs.

Formula	a (Å)	b (Å)	c (Å)	V ($Å^3$)
$CsPbI_3$	6.4270	6.4270	6.4270	265.467
$CsSnI_3$	6.2813	6.2813	6.2813	247.833
$CsGeI_3$	5.9992	5.9992	5.9992	215.916

3.2. Electrical properties

In this paper, GGA and mbj-GGA are used to simulate the total partial density of states of $CsMI_3$(M= Ge, Sn, Pb)under the equilibrium pressure of cubic perovskite phase[17]as shown in Figure. 3, where Fermi energy is zero reference point. Density of state describes the probability of electron distribution in the energy spectrum.

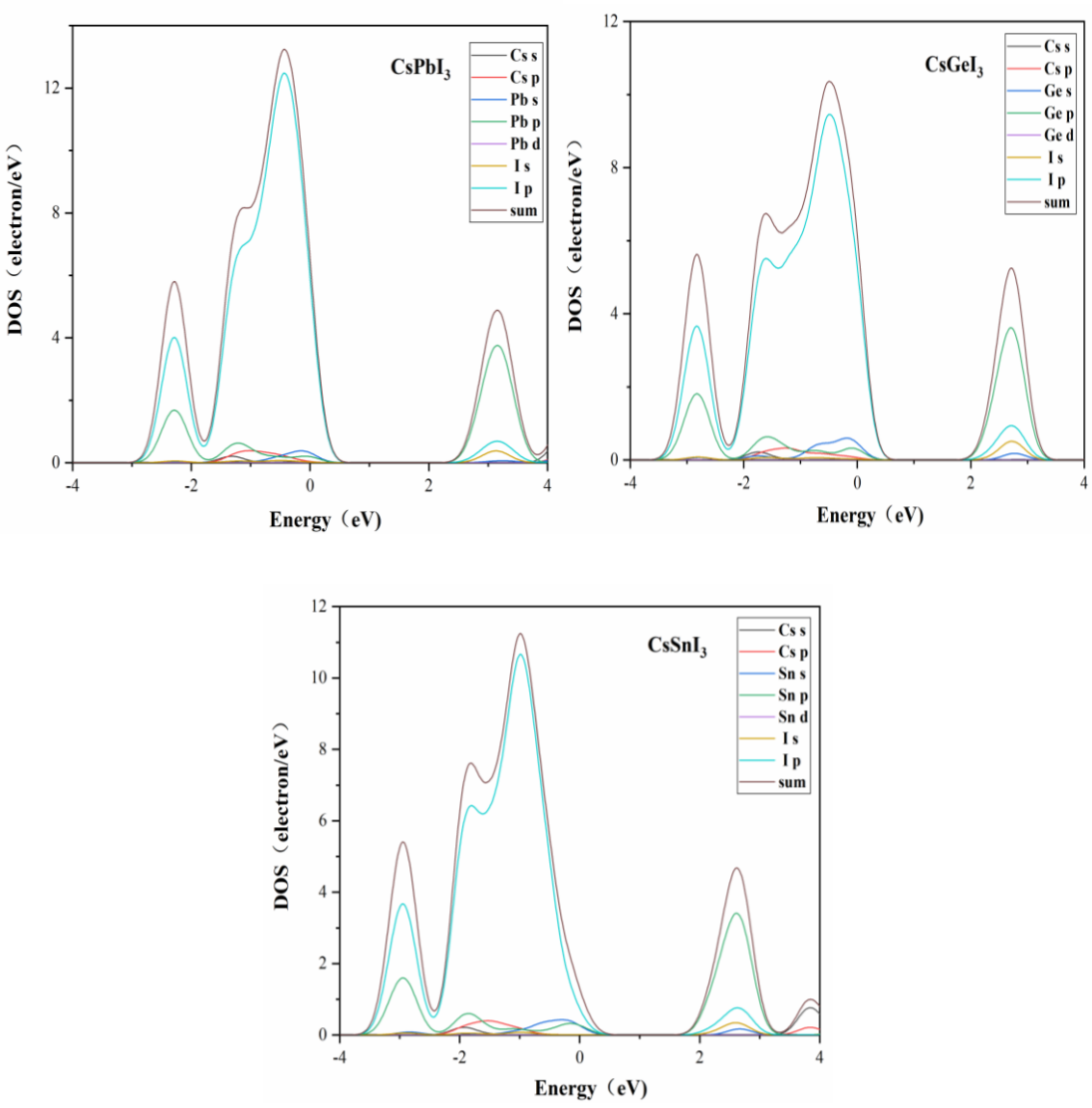

Figure 3: Calculated PDOS of $CsMI_3$(M=Ge, Sn, Pb)

According to the PDOS of $CsMI_3$(M= Ge, Sn, Pb), we can see the valence band(VB)edge of the $CsMI_3$(M= Ge, Sn, Pb)is mainly composed of the I-5p state, and the Pb-6p state contributes to the conduction band(CB)edge[18]. In the vicinity of Fermi surface, there is no peak in the density of state diagram of Cs element, that is to say, the contribution of positive monovalent metal cations Cs^+ to the band gap of the system is small, indicating that the probability of Cs^+ excited by photons is small[19]. There is no obvious coupling between Cs^+ and I^-, indicating that the interaction between Cs^+ and I^- is ion bond. So the band gap of $CsMI_3$(M = Ge, Sn, Pb)is mainly determined by M and I atom. At the top of the valence band, PDOS is mainly distributed around B and I atoms, while at the bottom of the conduction band, PDOS is mainly distributed around B(Ge, Sn, Pb)atoms[20]. This is to say that when the incident light irradiates the perovskite solar material, the 5s and 5p orbital electrons of B(Ge, Sn, Pb)are excited to transition to the 5p orbital of B(Ge, Sn, Pb)[21]. In this paper, we mainly study the influence of B-position on the band gap when B-position is a different element of the fourth main group. The energy band structure of $CsMI_3$(M= Ge, Sn, Pb) is shown in Figure 4. Each point on the abscissa in Figure 4 is the high symmetrical point in the Brillouin region. In the energy band diagram, the greater the fluctuation of energy band in the energy band diagram, the smaller the effective mass of electrons, the greater the degree of nonlocality, and the stronger the expansion of the atomic orbit that makes up this energy band. Such electrons generally belong to the sp orbit. On the contrary, the smaller band gap changes, the stronger the electron localization and the larger the electron effective mass. Generally, the energy bands near Fermi level are mainly analyzed, because these energy bands play a major role in determining the photoelectric properties of perovskite materials[22]. According to the figure, $CsMI_3$(M= Ge, Sn, Pb)are all direct band gap semiconductors, which are more suitable for photoelectric materials[23].The energy difference between VBM and Fermi level is much smaller than that between CBM and Fermi level, evidencing that these PVSKs are p-type semiconductors and the the main carrier is hole. The band gap value of $CsMI_3$(M = Ge, Sn, Pb)is consistent with the calculated value in the literature, but it is still smaller than the experimental value. This is because the pseudopotential underestimates the interaction energy between atoms, resulting in the low band gap value, which is common in the first principle calculation[24]. Generally, we can see the energy band structure diagram obtained by symmetry simplification, in order to fully express the energy level of the electron in the atomic orbit changing with the wave vector. In the first Brillouin region, the connection of special points of high symmetry is studied. Band gap is one of the main parameters that determine the application value of semiconductor. It represents the energy needed for the transition of electrons from the top of valence band to the bottom of conduction band. It is related to the attraction of bonding atoms to valence electrons. Figure 4 show the calculated band gap of $CsMI_3$(M= Ge,

Sn, Pb), where the $CsPbI_3$ band gap obtained by DFT(1.510eV)may has a difference on the experimental data. It is reported that, the experimental band gap data of $CsPbI_3$ quantum dot is 1.73eV[25]. Summarize the energy band structure of $CsMI_3$(M= Ge, Sn, Pb)in the Table 3. The band gap of ABX_3 PVSKs are known to increase with the Electronegativity of both B and X atoms. Electronegativity has now become one of the basic parameters in the study of material properties. It represents the ability of atoms in molecules to attract electrons to themselves[26]. Therefore, the properties determined by the ability of bonding atoms to attract electrons have a certain relationship with electronegativity. The electronegativities(in Pauling's empirical scale)of Sn, Ge and Pb are 1.96, 2.01 and 2.33, respectively, and band gap variation of the PVSKs follows the change of electronegativity[27]. It can be seen that, the band gap of $CsPbI_3$ is larger than $CsSnI_3$ and $CsGeI_3$, respectively, and the band gap also decrease with electronegativity decreasing.

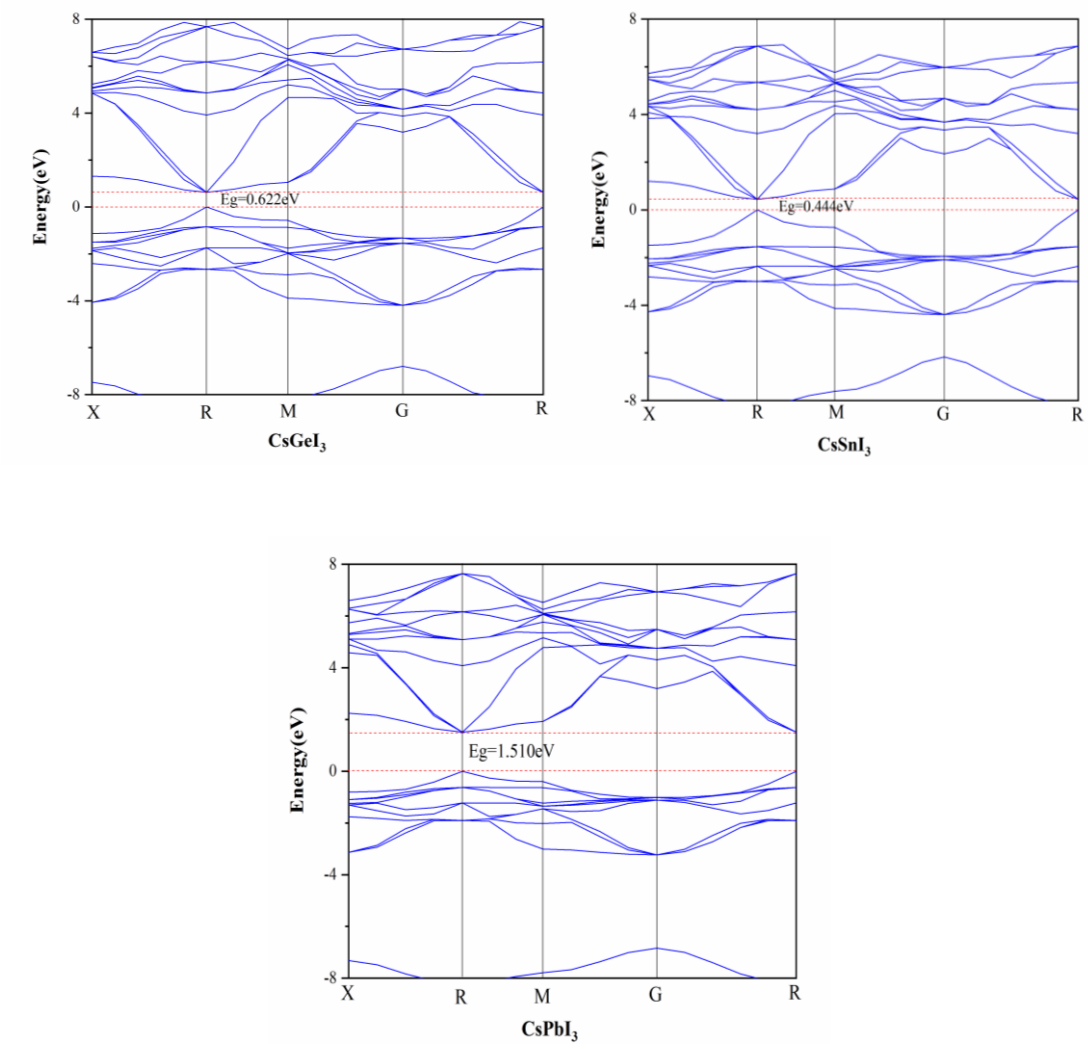

Figure 4: Band structure of $CsMI_3$(M= Ge, Sn, Pb)

Table 3: Calculated the energy band structure of $CsMI_3$(M= Ge,Sn,Pb)

Formula	$CsPbI_3$	$CsSnI_3$	$CsGeI_3$
Band gap(eV)	1.510	0.444	0.622

3.3. Optical properties

In this study, we calculated the optical absorption cofficient and the dielectric function of CsMI3(M= Ge, Sn, Pb) perovskite materials to study the response of CsMI3(M= Ge, Sn, Pb) perovskite materials under the ultraviolet and visible range. The simulated UV-vis absorption spectrum of CsMI3(M= Ge, Sn, Pb) are shown in Figure 5. Absorption peaks near 400nm blue-shift and in the visible range, Ge absorbs the most sunlight, followed by Sn and Pb. Sun light absorption increase with the decrement of atom radii[28]. In summary, the absorption of sunlight can be enhanced by replacing the Pb element with the smaller radius element of the fourth main group. In another word, Ge-replaced CsMI3 shows the best sun-light absorption property in the visible range.

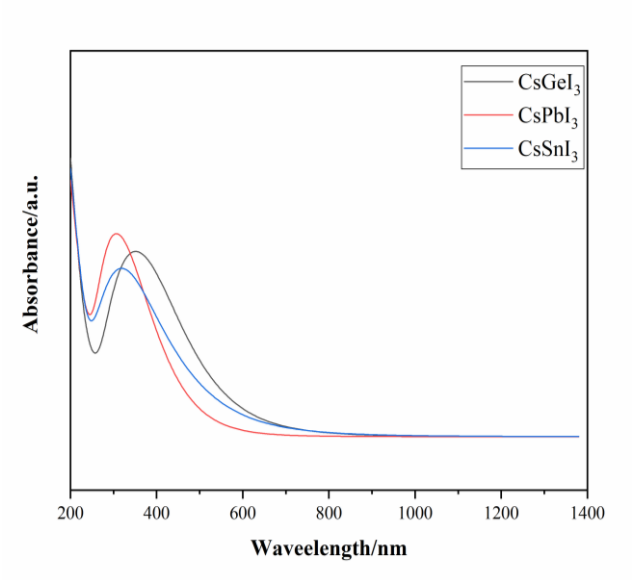

Figure 5: Simulated UV-Vis absorption spectrum of $CsMI_3$(M= Ge, Sn, Pb)

Dielectric function is also an essential factor in the study of light absorption, the optical absorption properties of the marerials can be expressed by the imaginary part (ε_2)of the relative dielectric function. ε_2 is directly proportional to the optical absorption capacity[29].The simulated Dielectric Function spectrum of CsMI3(M=

Ge, Sn, Pb) are shown in Figure 6. However, in this paper we only studies the properties of light absorption, so only the imaginary part of the dielectric function is considered[30]. As shown in the Figure 6, we can see that CsGeI3 has the strongest ability to absorb the sun light, in contrast, CsSnI3 has the weakest ability of light absorption.

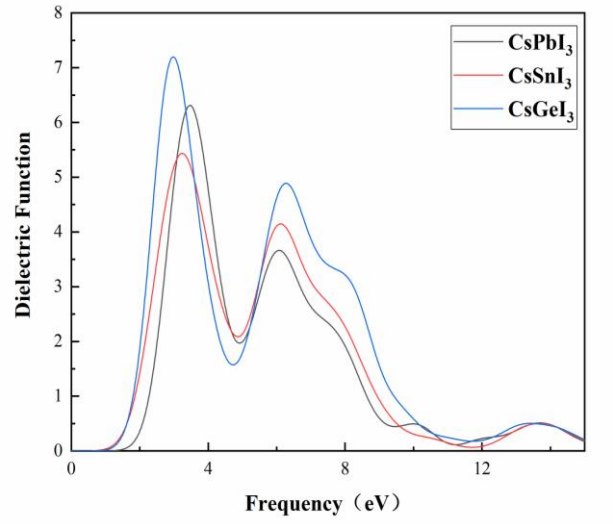

Figure 6: Simulated dielectric function spectrum of $CsMI_3$(M= Ge, Sn, Pb)

4. Conclusion

Replacing the Pb element of position B with the smaller radius element of the fourth main group can improve the stability of the material and reduce environmental pollution can be reduced. The crystal structure and electrical properties of CsMI3(M= Ge, Sn, Pb) material are calculated by density functional theory(DFT). The results showed that the band gap of the perovskite material decreases sharply after replacing lead elements with smaller radius of Ge and Sn. Narrow band gap absorb spectral energy that produces hot carriers and then relaxes, causing a lot of energy to lose in the form of heat.The best band gap of perovskite solar cell(PSKs) is 1.4eV. So the band gap for the production of solar cells, CsSnI3 and CsGeI3 is not as suitable as CsPbI3. However, through the absorption spectrum, it can be seen that in the visible light range, the absorption of sunlight is strongest when the element of the B site is Ge. By studying the imaginary part of the dielectric function, it can be concluded that CsGeI3 is more capable of absorbing sun light. Moreover, the tolerance factor of Ge element at B position is the highest of the three elements, which indicates that the stability of the material is the best. In conclusion, the light absorption capacity and stability have been greatly improved by replacing Pb element with elements of the fourth main group, and the environment pollution has also been reduced. If we want materials

that are more stable and have high efficiency and have lower Pb concentrations, we need to do some more elaborate doping work in the further and that's no longer covered.

Acknowledgements

This work was supported by National Natural Science Foundation of China, [grant number 61274064]

References

[1]. Kojima, A.; Teshima, K.; Shirai, Y.; Miyasaka, T. Organometal Halide Perovskites as Visible-Light Sensitizers for Photovoltaic Cells. Journal of the American Chemical Society. 2009, 131, 6050–6051.

[2]. Ning, Z. et al. Quantum-dot-in-perovskite solids, Nature. 2015, 523, 324–328.

[3]. Zhang, J.; Hodes, G.; Jin, Z.; Liu, S. All-Inorganic CsPbX3 Perovksite Solar Cells: Progress and Prospects. Angewandte Chemie International Edition. 2019, 58, 15596–15618.

[4]. Afsari, M.; Boochani, A.; Hantezadeh, M. Electronic, optical and elastic properties of cubic perovskite CsPbI3: Using first principles study. Optik. 2016, 127, 11433–11443.

[5]. Dong, Q.; Xia, X.; Zhang, B.; Wu, Y.; Dai, S. DFT modeling of ABX3 type perovskite doping structures. Acta Energiae Solaris Sinica. 2016, 37, 3086–3090.

[6]. Harmel, M.; Khachai, H.; Ameri, M.; Khenata, R.; Soyalp, F. DFT-based ab initio study of the electronic and optical properties of cesium based fluoro-perovskite CsMF3 (M=Ca and Sr). International Journal of Modern Physics B. 2012, 26, 1250199–1250211.

[7]. Padmavathy, R.; Amudhavalli, A.; Manikandan, M.; Rajeswarapalanichamy, R.; Iyakutti, K. Electronic and Optical Properties of CsSnI3−yCly (y = 0, 1, 2, 3) Perovskites: a DFT Study. Journal of Electronic Materials. 2019, 48, 1243–1251.

[8]. Jbara, A. S.; Munir, J.; Ul Haq, B.; Saeed, M. A. Density functional theory study of mixed halide influence on structures and optoelectronic attributes of CsPb(I/Br)(3). Applied Optics. 2020, 59, 3751–3759.

[9]. Vanderbilt, D. Soft self-consistent pseudopotentials in a generalized eigenvalue formalism. Phys. Rev. B. 1990, 41, 7892–7895.

[10]. Evarestov, R. A.; Kotomin, E. A.; Senocrate, A.; Kremer, R. K.; Maier, J. First-principles comparative study of perfect and defective CsPbX3 (X = Br, I) crystals. Physical Chemistry Chemical Physics.

2020, 22, 3914–3920 .

[11]. Even, J.; Pedesseau, L.; Jancu, J. M.; Katan, C. DFT and k Â· p modelling of the phase transitions of lead and tin halide perovskites for photovoltaic cells. Physica Status Solidi Rapid Research Letters. 2014, 8, 31–35.

[12]. Park, H. et al. Exploring new approaches towards the formability of mixed-ion perovskites by DFT and machine learning. Physical Chemistry Chemical Physics. 2019, 21, 1078–1088.

[13]. Lee, J. H.; Deng, Z.; Bristowe, N. C.; Bristowe, P. D.; Cheetham, A. K. The competition between mechanical stability and charge carrier mobility in MA-based hybrid perovskites: insight from DFT. Journal of Materials Chemistry C. 2018, 6, 12252–12259.

[14]. Marronnier, A. et al. Anharmonicity and Disorder in the Black Phases of Cesium Lead Iodide used for Stable Inorganic Perovskite Solar Cells. Acs Nano, p. acsnano. 8b00267. 2018, 12, 3477–3486.

[15]. Grote, C.; Berger, R. F. Strain Tuning of Tin-Halide and Lead-Halide Perovskites: A First-Principles Atomic and Electronic Structure Study. Journal of Physical Chemistry C. 2015, 119, 22832–22837.

[16]. Fang, Z. et al. Bandgap alignment of α-CsPbI3 perovskites with synergistically enhanced stability and optical performance via B-site minor doping. Nano Energy. 2019, 61, 389–396.

[17]. Jono, R.; Segawa, H. Theoretical Study of the Band-gap Differences among Lead Triiodide Perovskite Materials: CsPbI3, MAPbI3, and FAPbI3. Chemistry Letters. 2019, 48, 877–880.

[18]. Liu, D.; Li, S.; Fang, B.; Meng, X. First-Principles Investigation on the Electronic and Mechanical Properties of Cs-Doped CH3NH3PbI3. Materials. 2018, 11, 1141–1151.

[19]. Paduani, C.; Rappe, A. M. Tuning the gap of lead-based halide perovskites by introducing superalkali species at the cationic sites of ABX3-type structure. Physical Chemistry Chemical Physics Pccp. 2017, 19, 20619–20626.

[20]. Song, G.; Gao, B.; Li, G.; Zhang, J. First-principles study on the electric structure and ferroelectricity in epitaxial CsSnI3 films. Science. 2017, 7, 41077–41083.

[21]. Wan, J. et al. Unique Properties of Halide Perovskites as Possible Origins of the Superior Solar Cell Performance. Advanced Materials. 2014, 26, 4653–4660.

[22]. Rahman, N. M.; Adnaan, M.; Adhikary, D.; Islam, M.; Alam, M. K. First-principles calculation of the optoelectronic properties of doped methylammonium lead halide perovskites: A DFT-based study. Computational Materials Science. 2018, 150, 439–447.

[23]. Stoumpos, C. C.; Malliakas, C. D.; Kanatzidis, M. G. Semiconducting Tin and Lead Iodide Perovskites

with Organic Cations: Phase Transitions, High Mobilities, and Near-Infrared Photoluminescent Properties. Inorganic Chemistry. 2013, 52, 9019–9038.

[24]. Yang, Y.-Y.; Wang, L. S.; Xu, W. K.; Zhang, Y.; Chen, F. X. Simulation Optimizing Planar Heterojunction Perovskite Solar Cells with CsGeI3 as Hole Transport Materials. Journal of Synthetic Crystals. 2017, 46, 814–819.

[25]. Giorgi, G.; Fujisawa, J. I.; Segawa, H.; Yamashita, K. Cation Role in Structural and Electronic Properties of 3D Organic–Inorganic Halide Perovskites: A DFT Analysis. Journal of Physical Chemistry C. 2014, 118, 12176–12183.

[26]. Hong, J.; Stroppa, A.; Iniguez, J.; Picozzi, S.; Vanderbilt, D. Spin-phonon coupling effects in transition-metal perovskites: A DFT + U and hybrid-functional study. Physical Review B Condensed Matter. 2011, 85, 054417–054428.

[27]. Zhou, J.; Fan, W.; Zhou, Q.; Wu, K.; Cheng, Y. DFT studies of electronic structure and dielectric properties in layered perovskite. Journal of Computational Electronics. 2016, 15, 466–472.

[28]. Leupold N.; Scho¨tz K.; Cacovich, S. et al. High versatility and stability of mechanochemically synthesized halide perovskite powders for optoelectronic devices. ACS Appl Mater Interfaces. 2019, 11, 30259–30268.

[29]. Ghebouli, M. A.; Ghebouli, B.; Fatmi, M.; Bouhemadou, A. Calculation of physical properties of the cubic perovskite-type oxide using the PP-PW method based on the DFT theory. Solid State Communications. 2011, 151, 908–915.

[30]. Polman, A.; Knight, M.; Garnett, E. C.; Ehrler, B.; Sinke, W. C. Photovoltaic materials: Present efficiencies and future challenges. Science. 2016, 352, 4424–4434.